Incorporating damping predictions in the vibroacoustic design process.

Etienne Balmes

SDTools, 44 Rue Vergniaud, 75013 Paris, France

Ecole Centrale Paris, MSSMat, 92295 Chatenay Malabry, France

balmes@sdtools.com

Abstract

Controlling vibration amplification phenomena is a critical aspect of structural dynamics. Innovative devices, such as SPADD® are now available, that allow much better damping performance than classical free and constrained layer treatments. The current practice in vibration design does not however incorporate damping modeling so that a new range of tools is needed. The paper first presents functional models of SPADD® devices and discusses applicable placement strategies. In a second part, one analyzes optimization strategies that can be considered in the design of damping treatments. First one presents the necessary trade-off between rapid estimates, needed in a phase where the damping potential is to be evaluated, and more costly estimates, needed in design refinement. It shown that very appropriate trends can be obtained using fast approximations implemented in the ProSPADD software package. The need to define appropriate objective functions is then discussed. Illustrations are given using the simplified model of a body in white with two treatments targeting the first torsion and a panel mode respectively.

1   Introduction

Resonance amplification phenomena are the source of most problems in vibration and acoustic performance. Their control is thus key in aerospace and automotive applications and increasing damping is one of the main solutions. Free and constrained viscoelastic treatments are well established damping techniques, but more efficient solutions can very often be obtained by combining mechanical amplification and constrained layer damping. Figure 1 illustrates such concepts with two SPADD® damping solutions developed by ARTEC Aerospace.
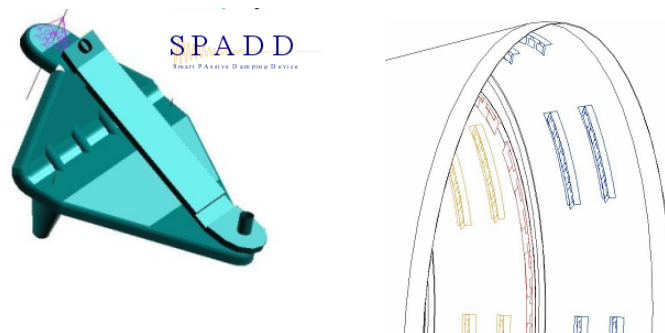

Figure 1: SPADD® struts (engine mount) and lineic devices (aircraft radar shield)

The performance of damping devices is directly linked to their placement and their properties relative to the modes of the supporting structure. As a result, numerical optimization is a necessary design step. While

standard design methodologies address mass and stiffness design, damping analyses are typically confined to validation phases. Introducing practical damping design methodologies is thus a critical step to augment the use of damping technologies.

This study builds on efforts to validate the ProSPADD [1] software package and on other more fundamental developments [2, 3, 4]. The key requirement for ProSPADD is that it allows a rapid evaluation of the damping potential of damping treatments based on SPADD® technology. It must provide reliable predictions of damping potential early in a project cycle so that design refinement can take place in due time.

Section 2 presents the functional models of the three basic damping treatments considered in ProSPADD (struts, lineic and patch devices) and gives the base concepts underlying the placement algorithms that have been implemented.

The rest of the paper addresses some key issues in damping design. Section 3.1 motivates the need for numerical optimization and gives details on the example (the simplified model of a body in white). Section 3.2 discusses the level of approximation needed for damping evaluation. It is shown that the estimates based on real modes used in ProSPADD are sufficient for pre-design. Section 3.3 considers a higher frequency region where the number of modes limits the usefulness of damping ratio as objective functions. Strategies for the use of target transfers are thus discussed.

2   Modeling and placing damping devices

2.1   Equivalent modeling of basic damping devices

Damping struts are point to point connections. They are typically meant to act as pinned bars although in reality they also transmit moments and for long struts tend to have their own internal modes. The simplified model shown in figure 2 represents the feet (connections between the underlying surface and the main strut line) as beams and the strut as a simple sandwich with the bottom and top layers connected to the left and right foot. While the technological implementation can be quite different, this model captures the basic characteristics of damping struts : damped traction/compression spring, offset of the spring axis with respect to the support surface, possible transmission of moments.
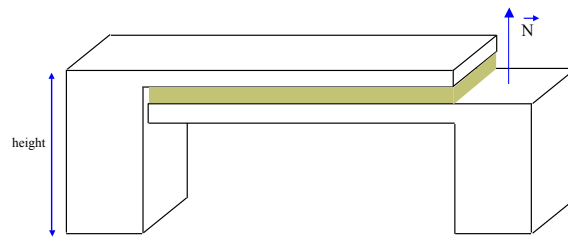

Figure 2: Functional model of damped strut

SPADD-T devices are in line assemblies of simple patterns as illustrated in figure 1. The model retained for one pattern represents the frames (shown in white in figure 3) as shell elements and assumes a viscoelastic that covers the entire surface of between the feet. This is again a functional model used for initial design.
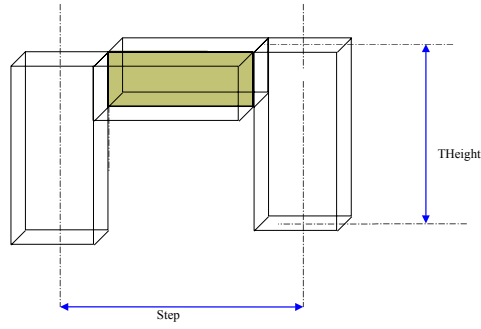
Figure 3: Functional model of a SPADD-T pattern

SPADD® Patch devices generalize the standard constrained layer treatments by adding small blocks, that increase the offset between the free surface of the supporting structure and the constrained layer, and allow for beneficial discontinuities in the shear strain in each connected area.
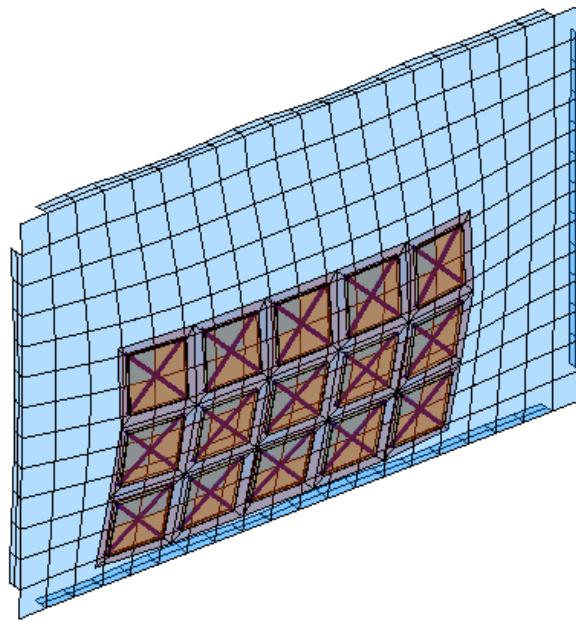

Figure 4: Mesh for a SPADD® Patch surface device with square offset blocks

In a practical pre-design strategy, it is not acceptable to remesh the supporting structure. Meshing strategies in ProSPADD are thus based on reference meshes of the various devices that are parameterized in geometry, and mapped onto the surface of the original mesh. Most of the time, the result is not conform. The connection, between the damping treatment and the supporting structure, is obtained using linear multiple point constraints generated with underlying shape functions of the supporting elements. The reference models used standard shell/volume/shell models discussed in Ref. [3].

2.2 Placement strategies

Figure 5 illustrates energy localization in basic damping mechanisms. As a surface bends, lines with an offset with respect to the surface neutral axis elongate. Free layer damping treatments (shown on top in figure 5) elongate with the free surface of the supporting structure. Strain, and thus energy dissipation, peak where the surface curvature is maximum (in the figure at the center of the bending beam).

Constrained layer damping treatments have a different principle. Two surfaces bend but a differential elongation is generated by the different neutral axes. The constrained shear layer is thus stressed significantly to minimize the relative displacement of the two connected surfaces. High levels of shear are now found away from the maximum curvature areas, where the differential motion of the two surfaces is maximum. Constrained layer treatments are thus inherently sensitive to global properties of the structure (how the different surfaces are connected, their dimensions, boundary conditions, etc.) which makes their positioning and design much more difficult.

SPADD-T treatments carry load uniquely through the viscoelastic layers. They thus have an overall behavior that is similar to that of free layer treatments, as confirmed by the localization of energy dissipation in figure 5.
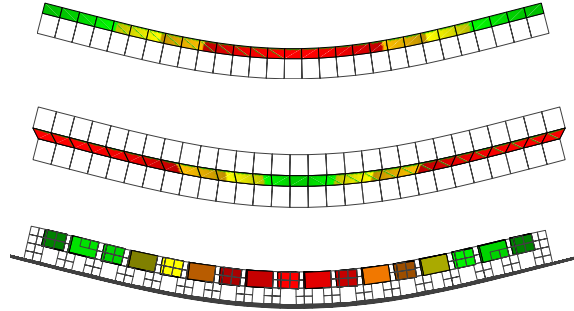

Figure 5: Localization of dissipation in standard viscoelastic damping devices

Since SPADD-T efficiency is directly linked to surface elongation at a certain distance from the neutral axis, one can compute principal strains of a membrane placed at that distance. The value of the principal strain gives a damping potential at a particular location, while the principal direction gives the optimal orientation for a SPADD-T pattern.

Figure 6 illustrates this strain map building for a simple beam like structure with a hole and the resulting placement using the incremental placement strategy implemented in ProSPADD. Such automation is a significant help in building efficient damping designs.
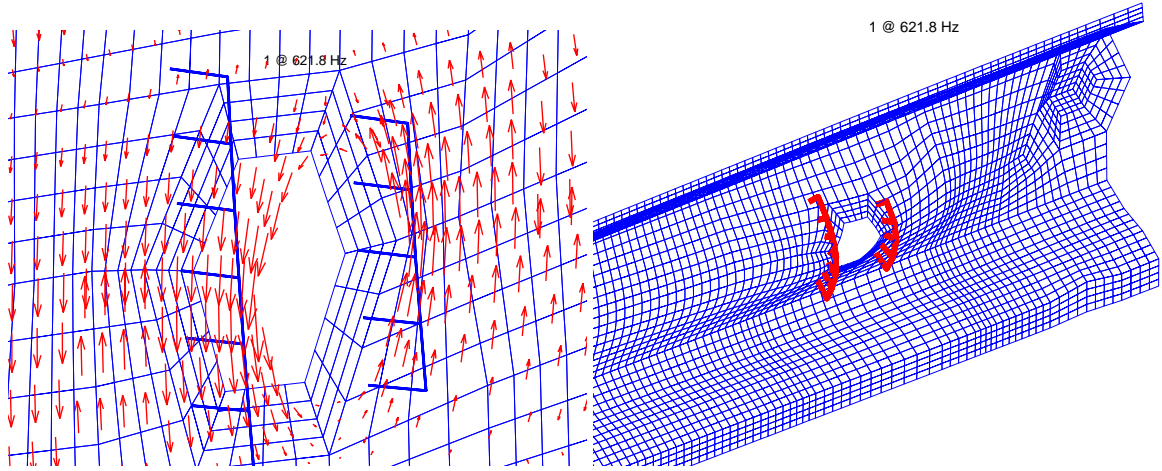
Figure 6: Strain maps and resulting device placement

The placement of patch treatments is more difficult since the key parameter is the differential elongation of two surfaces, which is a quantity that needs to be integrated over a certain distance (the surface of the constraining layer). Currently placement is thus performed manually using heuristic rules.

3 Parametric optimization

3.1 Principles

For all functional designs, damping performance is strongly dependent on the relative stiffness of base structure and the damping devices. The stiffness of the viscoelastic shear layers is essentially equal to $k_v = GS/h$ where the modulus G depends on the material selection, the viscoelastic surface S and thickness h. The last two being fairly open design parameters, k_v can be selected in a very wide range of values (several orders of magnitude).

It is important to distinguish the pre-design phase where a nominal value of G is used with a constant loss factor (typically 1) and the validation phases where the nomogram of the material is considered to validate performance over a frequency/temperature range [3]. To determine a k_v during pre-design, one assembles the matrices for the elastic K_e and viscoelastic K_v parts and considers the parameterized dynamics stiffness given by

$$[Z(k_v, s)] = \left[Ms^2 + K_e + \frac{k_v}{k_{v0}}[K_v] \right] \tag{1}$$

One then seeks to optimize k_v. This optimum can be judged using root locus plots (shown in figure 7) where one displays the complex poles associated with (1).
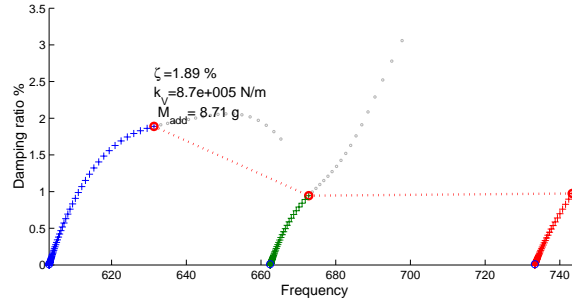
Figure 7: Locus of poles when changing the viscoelastic treatment equivalent stiffness.

Locus plots are easily used for the first few modes of a structure where the number of modes in the band is limited and one can easily track modes of interest. At higher frequencies, estimating the impact of the treatment would at least imply having a very efficient method to track poles through complex changes. As discussed in section 3.3, one then prefers to analyze target transfers $\{y\} = [c][Z^{-1}][b]\{u(s)\}$.

The parametric optimization phase will be illustrated using the simplified model of a body in white. This model is representative of car body dynamics but was chosen small (105 000 DOF, 20 000 elements) to allow for fast evaluations of exact solutions needed in the methodology validation phases discussed here.

Two damping designs are chosen to illustrate objectives for the first few modes or a larger band. Four struts, shown in red in figure 8, are placed to damp the first torsion mode. Adjustments can actually be made to damp the first bending mode too but these were not considered in the present study that seeks to validate numerical methods. A patch treatment is placed on a rear panel with the objective to illustrate a noise radiation objective at higher frequencies.
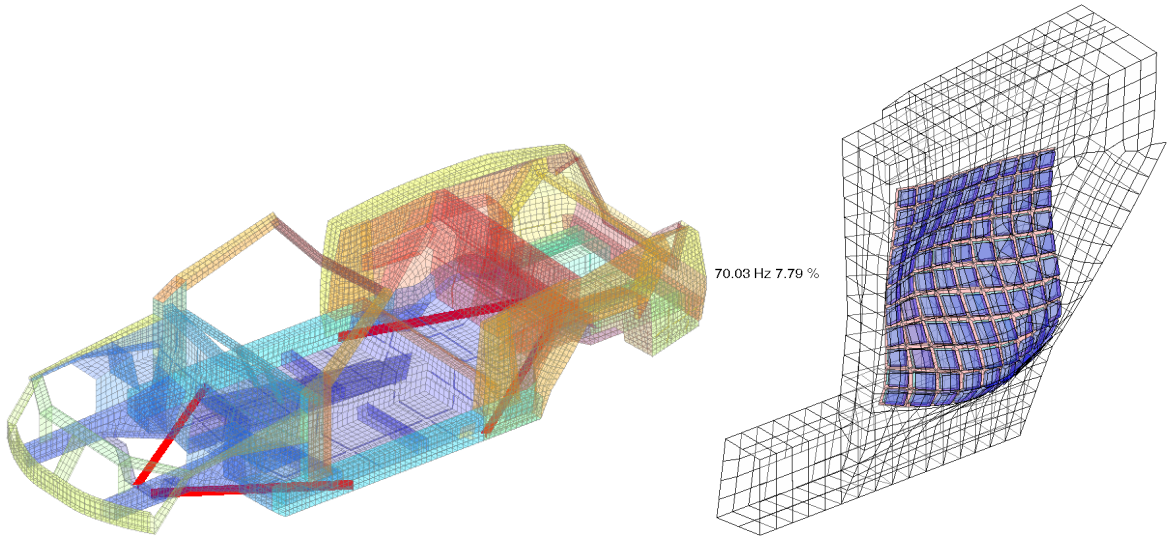

Figure 8: Example of a simplified car body in white. Damping struts for torsion mode damping. Patch treatment at the rear for higher frequencies (the first panel mode with significant damping is shown).

3.2 Approximate solvers

The objective of this section is to analyze the level of approximation needed to perform the parametric optimization phase. In a design phase, it is highly desirable to determine reasonable results for the optimal

viscoelastic stiffness in a matter of minutes. Complex eigenvalue solution for a realistic model of an auto-motive body will take several hours, if it converges at all (complex eigenvalue solvers are significantly less robust than real ones). A practical design methodology thus needs both higher robustness and computational speedup by orders of magnitude.

Ritz-galerkin analyzes, also known as model reduction, give general framework for such solvers [5]. One seeks the solution within a subspace T. For complex modes, one thus solves

$$[T]^T\Big[M\lambda_j^2 + K_e + \tfrac{k_v}{k_{v0}}[K_v]\Big][T]\{\psi_{jR}\} = \{0\} \tag{2}$$

and the resulting eigenvector can be recovered on all degrees of freedom by $[T]\{\psi_{jR}\}$.

The classical *modal solution* uses a basis $T = [\phi(k_v)_{1,NM}]$ containing a certain number of real modes computed for a given value of k_v (this is for example implemented as SOL110 in NASTRAN and is an extension of the Modal Strain Energy method [6]). The following extensions were considered in this study:

(A) for initial placement of the damping treatment, modes of the untreated structure are the only available. One thus approximates the damped behavior of the structure using those modes by condensing the models of the added damping devices onto the DOF of the untreated model. The underlying motivation for this approximation is that the impact in terms of mass and stiffness is relatively marginal compared to the induced damping. This approximation is the basis of the placement phase in ProSPADD.

(B) once devices placed and target value of k_v determined, one can recompute normal modes $T = [\phi(k_v)_{1,NM}]$ and use these to validate the retained configurations. While the typical objective is to validate the accuracy of predictions at this particular value of k_v, one may want to use these to restart an optimization of k_v. This approximation is the basis of the validation phase in ProSPADD.

(C) the last approximation considers the first order correction $T = \begin{bmatrix} \phi(k_v)_{1,NM} & K_0^{-1}K_v\phi(k_v)_{1,NM} \end{bmatrix}$ introduced in Ref. [7, 5]. First order approximations are currently only accessible through the *viscoelastic tools* [4] and thus cannot be easily incorporated into ProSpadd [1]. They induce acceptable computational costs but their range of validity needs to be tested.

Figure 9 shows the locus of the torsion and bending modes of the body in white example as k_v is varied for the four struts.
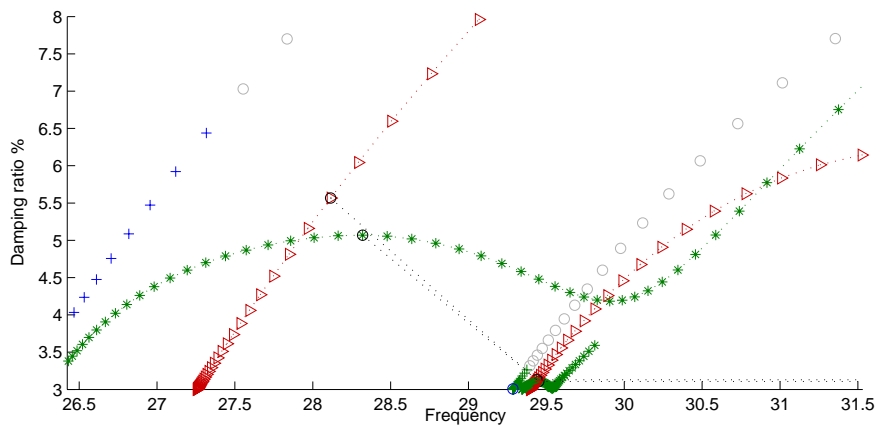

Figure 9: Estimated root locus with various approximations (body in white, four damping struts) + and grey ∘ approximation (A), ▷ approximation (B), ∗ approximation (C).

The lines with + and ∘ markers are the initial estimates (A) based on untreated modes of the structure. They correctly indicate a significant damping impact on the torsion mode. But the effect on the bending

mode (near 29 Hz) seems to be significant. For this configuration of the struts, exact computations however show a marginal impact. In the plot, the transition from $+$ to $\circ$ indicates that the confidence in the prediction becomes poor. Using this indication, one sees the confidence is poor on the damping increase for the bending mode. The initial diagram is thus an acceptable design tool.

If modes are computed around a given k_v, the modal approximation (B) is retained to validate the actual performance of the design. The root locus generated with these modes is shown in red with $\triangleright$ markers and the poles at the retained value of k_v are marked with $\circ$ and connected by dotted lines. One can also create a reduced model with first order correction using $K_0 = [K_e] + k_{v0}[K_v]$ and the associated root locus is show in green with $*$ markers.

The value at the design point (black $\circ$ markers) are very close in both approximations, but when the reduced basis is used to build a root locus, one sees that the modal approximation (B) gives poor indications (in particular the frequency no longer converges to the correct value for small k_v). This implies that the k_v range where approximation (B) is meaningful is actually smaller than that of (A).

Finally, the first order approximation also shows a surprising rise in damping for high values of k_v. Figure 10 compares this approximation modal estimates for variable values of k_v (the normal modes are computed at each point rather than just once at the target value of k_v shown with red $\circ$). One clearly sees that the sharp rise is associated with a limitation of the first order approximation. This illustrates a systematic trend in first order approximations (also shown in Ref. [3]): they often fail for significantly larger values of the parameter. As a consequence, they are thus generally better if the point at which they are built corresponds to a high value of the variable parameter.
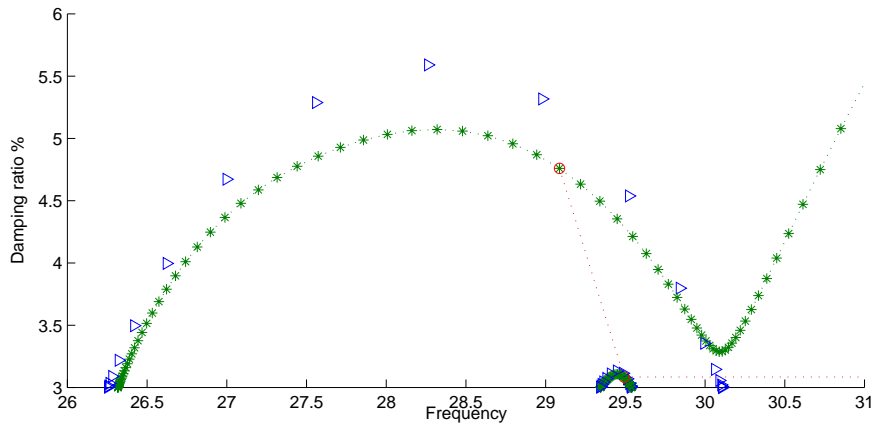

Figure 10: First order $*$ and modal estimate $\triangleright$ at various values of k_v (body in white, four damping struts).

3.3 Objective functions

In this section, one validates the applicability of objective functions that can be retained to optimize the damped behavior at higher frequencies. The example chosen is the patch treatment shown in figure 8. This treatment is meant to damp a particular panel mode and is thus of interest at higher frequencies. In this particular example there are 40 modes below 90 Hz and only two involve significant contributions of the target panel.

Figure 11 illustrates the fact that tracking modes becomes difficult. As expected most modes are not significantly damped and only two show a major damping (viscous damping ratio up to 10 %). This diagram also shows that damping is achieved with significant frequency shifts of the target modes so that tracking modes by order is not appropriate.
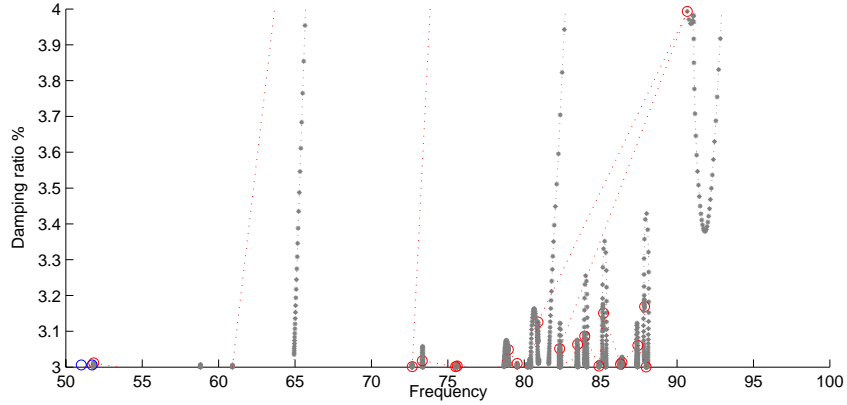
Figure 11: First order estimate of locus for patch treatment.

In practice, it thus appears that the locus plots are difficult to manipulate when dealing ranges with significant modal density. Computing target transfer functions is an alternative. Figure 12 illustrates the effect of changing the stiffness of the patch viscoelastic. The transfer was selected to enhance the contribution of the treated panel peak near 65 Hz at low values of k_v. As apparent in the locus plots and the transfers, other modes are not very affected by the treatment.

For low values of k_v the peak associated with the target mode is clearly dominant so that tracking it's evolution is simple. One sees that a value of k_v/k_{v0} near to 1 is needed to achieve significant damping. Determining the exact optimal value is however difficult because these curves lack the direct interpretation of a scalar objective function.
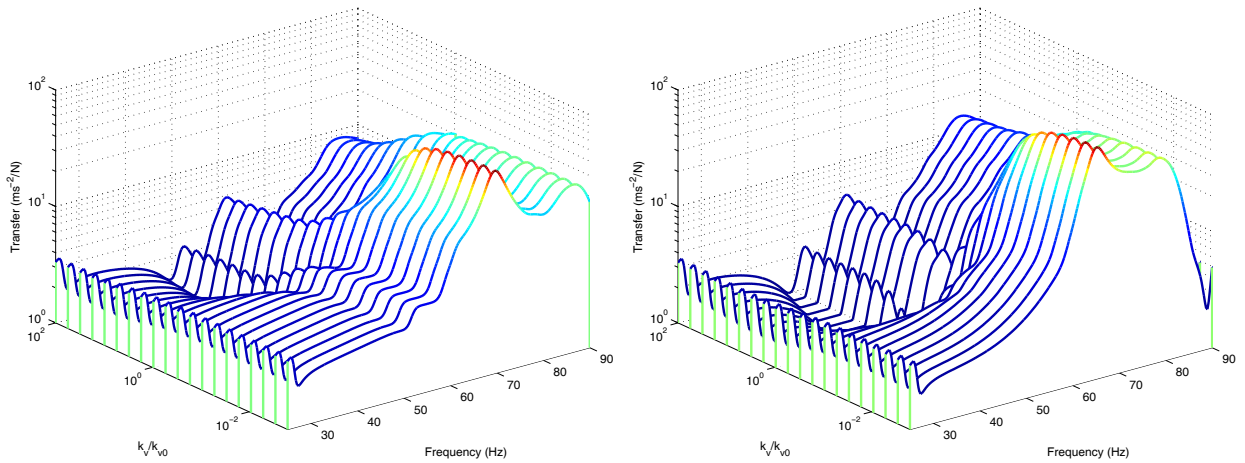

Figure 12: Transfer from rear wheel mount to center of treated pannel. **Left:** Modal approximation (A). **Right:** first order approximation (C).

One idea would be to track peaks, which is similar to specifying a target mode but simpler in the sense that you don't need to know its number. The resulting plot is shown in figure 13. As the target mode becomes significantly damped, other peaks begin to appear in the transfer function and it becomes more difficult to determine whether increasing the viscoelastic layer stiffness is appropriate or not.
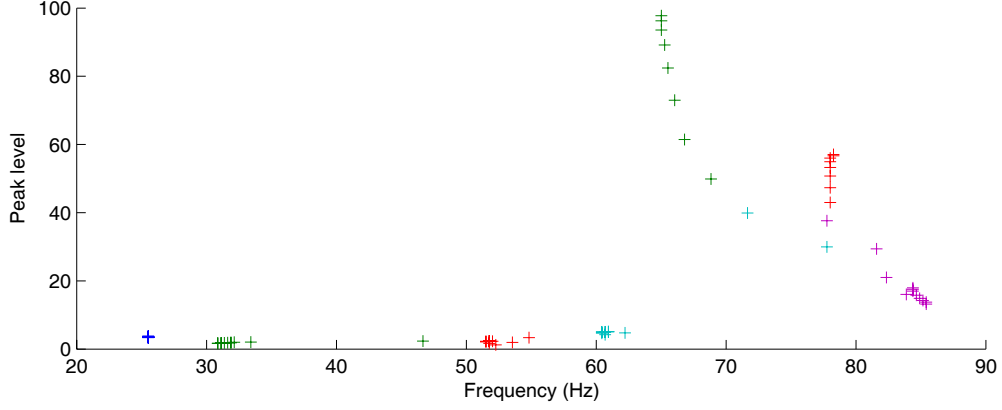

Figure 13: Peak tracking on transfer functions.

Another classical approach is to integrate the response over a given frequency band with possibly a weighting function $w(\omega)$

$$J(H) = \int_{\omega_{\min}}^{\omega_{\max}} w(\omega) H(\omega) H^H d\omega \tag{3}$$

This is illustrated in figure 14. Again, one clearly sees the need to increase k_v/k_{v0} up to a value near to 1. In this particular case the RMS value continues to decrease. While the reason for the decrease will be explained later, this is a common feature that makes the automated selection of the optimum difficult.

This plot also illustrates differences between the modal and first order approximations. The error is however relatively small at the k_v/k_v0 point where the approximation was built (indicated as a vertical dotted line). Away from that area, the modal approximation (B) significantly underestimates RMS levels (in other words the effect of the damping treatment is overestimated). This confirms the relatively narrow range of validity for approximation (B). Other studies have also shown that, for low damping levels, approximation (B) is poor even at the current point.
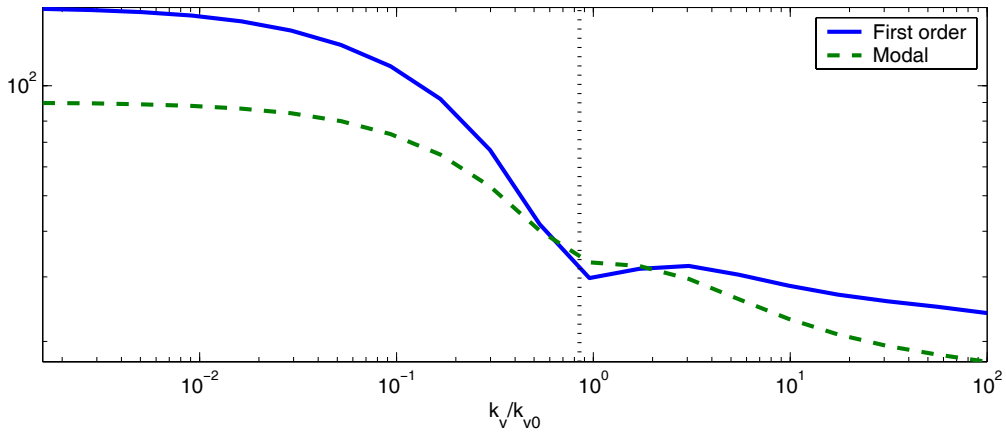

Figure 14: Predictions of the RMS response of one target transfer function.

Part of the difficulty in interpreting transfer function results is due to the arbitrariness in the selection of the output point. It is thus interesting to aggregate responses predicted at multiple points using standard Mode Indicator Functions developed for experimental modal analysis: sum of absolute values, sum of squares of imaginary parts, CMIF [8]. Figure 15 shows the sum of the imaginary parts of responses on nodes of the damped panel for two input locations.

For an horizontal input (graph on the left), the panel mode is dominant. The peak tracking clearly shows the effect of the amplitude decrease as the mode gets damped. Increasing k_v/k_v0 above 1 induces a major frequency shift and the target mode actually gets out of the range which explains the continued decrease of the RMS value.

For a vertical input (graph on the right with a narrower frequency range), the increased damping is actually associated with a rise in peak level due to coupling with the 73 Hz mode.

Defining transfer based design strategies thus remains a fairly open subject and heuristic methods are currently used.
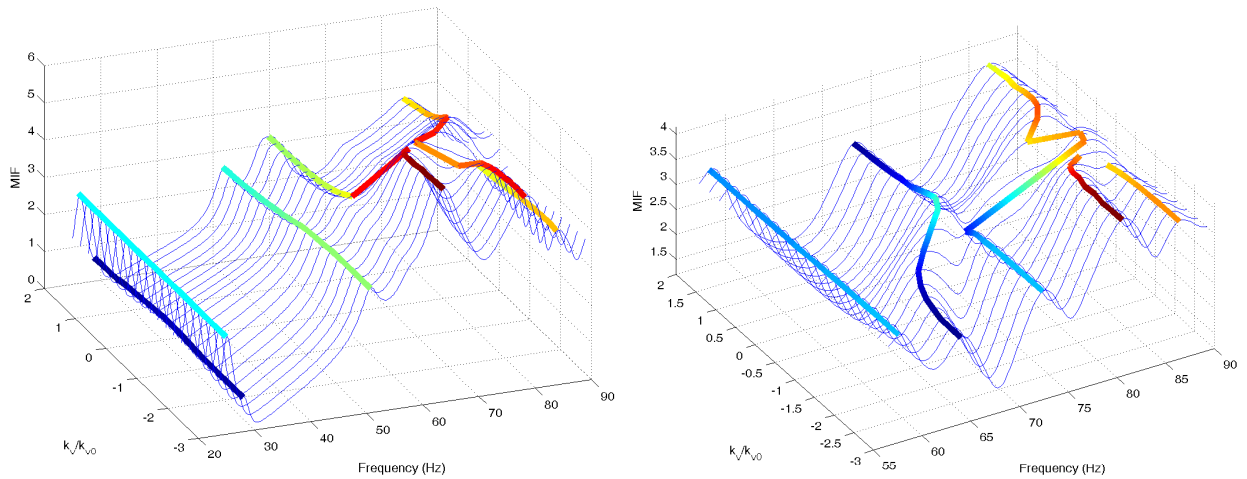

Figure 15: Sum of imaginary parts of the response on the surface of the patch. **Left:** y input on the rear wheel. **Right:** z input on the front wheel.

4 Conclusion

Model reduction techniques have been implemented that allow practical damping design studies. The modal approximations used by the ProSPADD software have been shown to be well adapted for pre-design phases, where one seeks to evaluate the damping potential of various treatments. Evaluations of higher order approximations that would be considered in design refinement phases have also been made. These integrated tools open the way to the incorporation of damping predictions in the structural design cycle. The introduction of innovative damping devices opens new trade-offs : for example replacing stiffeners by simple distributed damping treatments. One can thus expect the design in a shorter cycle of lighter and simpler structures.

References

[1] Balmès, E., *ProSpadd User's Manual*, SDTools and Artec Aerospace, 2004.

[2] Kergourlay, G., *Mesure et prédiction de structures viscoélastiques - Application à une enceinte acoustique*, Ph.D. thesis, Ecole Centrale de Paris, 2004.

[3] Balmès, E. and Germès, S., "Design strategies for viscoelastic damping treatment applied to automotive components," *IMAC, Dearborn*, 2004.

[4] Balmès, E., *Viscoelastic vibration toolbox*, SDTools, 2004.

[5] Bobillot, A., *Méthodes de réduction pour le recalage. Application au cas d'Ariane 5*, Ph.D. thesis, Ecole Centrale de Paris, 2002.

[6] Rogers, L., Johson, C., and Keinholz, D., "The Modal Strain Energy Finite Element Method and its Application to Damped Laminated Beams," *Shock and Vibration Bulletin*, Vol. 51, 1981.

[7] Plouin, A. and Balmès, E., "Steel/viscoelastic/steel sandwich shells. Computational methods and experimental validations." *International Modal Analysis Conference*, 2000, pp. 384–390.

[8] Phillips, A. W., Allemang, R. J., and Fladung, W. A., *The Complex Mode Indicator Function (CMIF) as a parameter estimation method*, International Modal Analysis Conference, 1998.